

Structure and Electrical Properties of Zirconium-Doped Tin-Oxide Films

A. V. Sitnikov^a, O. V. Zhilova^{a*}, I. V. Babkina^a, V. A. Makagonov^a,
Yu. E. Kalinin^a, and O. I. Remizova^a

^a Voronezh State Technical University, Voronezh, 394026 Russia

*e-mail: zhilova105@mail.ru

Submitted December 21, 2017; accepted for publication February 5, 2018

Abstract—Thin Zr-stabilized SnO₂ films are fabricated by ion-beam reactive sputtering. The amorphous thin-film SnO₂ samples with various Zr concentrations are synthesized in a single production process. The influence of heat treatment on the structure and electrical properties of the synthesized films is studied. The onset of crystallization in thin-film Sn–Zr–O systems is observed at 673 and 773 K, which is accompanied by the appearance of metastable phases. Being heated to 873 K, these phases are transformed into Sn + Sn₂O₃. It is found that the electrotransfer the film crystallization at temperatures close to room temperature is thermally activated with an activation energy of ~0.78 eV. Tin-oxide films doped with Zr from 0.6 to 3.9 at % manifest the property of hydrogen-gas sensitivity after crystallization.

DOI: 10.1134/S106378261809018X

1. INTRODUCTION

Tin oxide, being a wide-gap semiconductor, possesses an interesting combination of properties such as transparency in the visible range of electromagnetic radiation, high electrical resistance, and high gas sensitivity. Such properties facilitate the broad practical application of SnO₂ as solar cells, gas sensors, and other electronic devices [1–3]. Despite the similarity with other wide-gap semiconductors, tin oxide has a series of peculiarities. In many cases, we can assume that the crystal lattice of tin oxide consists of metal cations and oxygen anions, due to which, such defects as vacancies and interstitial atoms are charged and electrically active, i.e., they can manifest both donor and acceptor properties. However, undoped SnO₂ possesses only the electronic type of conductivity [4].

Despite the great attention from physicists and materials scientists in studying tin oxide, the nature of many experimentally observed peculiarities of its electrical properties remains unclear [5, 6]. For example, the gas sensitivity of tin-oxide thin films is determined by processes on the grain surface affecting the electrical conductivity of the film [7]. Tin oxide has a high resistivity and a wide band gap of ~3.5 eV; therefore, almost no increase in the intrinsic conductivity of the semiconductor occurs at elevated temperatures (~673 K) [8–10].

Polycrystalline tin oxide with nanoscale grains, whose electrical conductivity increases because of numerous defects in the grain-boundary layer, is used to decrease the electrical resistance. Herewith, several

problems appear. First, the finely dispersed crystal structure should be stabilized because recrystallization starts at high temperatures. Second, the presence of doping additives changes the energy states of carriers [11, 12]. All these circumstances affect the mechanisms of varying the surface charge density during the adsorption of atoms and molecules of various gases.

To solve these problems, thin-film samples are usually used, which makes it possible to increase the contribution of surface states to the electrical-transport properties of a semiconductor.

One method of obtaining nanocrystalline SnO₂ films is controlled crystallization from the amorphous state, to form which, amorphizing refractory metals are used. The latter slow crystallization during heat treatment and stabilize the nanocrystalline structure, which affects the surface energy states of carriers at the interface between the crystallites.

In this study, we selected zirconium (Zr) as the amorphizing additive. This is due to the following reasons: zirconium is the element used to form the amorphous structure of a wide class of alloys; Zr can be a catalyst during the interaction of hydrogen with SnO₂; ZrO₂ has a high melting point, and therefore prevents an increase in the grain size during the crystallization and recrystallization of the structure upon heat treatment.

Thus, the use of Zr as the doping element in SnO₂ compound makes it possible to reveal the influence of various factors on the electrical and sensing properties of tin oxide.

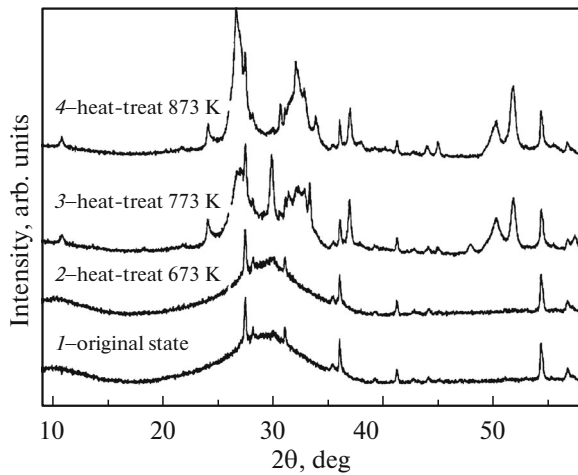


Fig. 1. X-ray diffraction patterns of Sn–Zr–O films (Zr = 3.9 at %) in the initial state (curve 1) and after heat treatment for 30 min at temperatures of 673 K (curve 2), 773 K (curve 3), and 873 K (curve 4).

2. SAMPLES AND EXPERIMENTAL

Thin SnO₂ films stabilized with Zr were fabricated by ion-beam reactive sputtering [13]. To form the thin-film structure, tin oxides with a high zirconium concentration were used as a composite target, which was a tin-based cast 280 × 80 mm in size, on the surface of which, five zirconium plates 80 × 9 × 2 mm in size were fastened. The distance between the zirconium plates gradually varied from 5 mm on one target end to 45 mm on the other end, which allowed us to obtain various ratios of the Zr concentration depending on the substrate position relative to the target in one process cycle.

We used argon (Ar) of purity 99.992% as the main working gas. The working gas was continuously supplied into the chamber during the production process. The working chamber was pumped to a pressure of no higher than 1×10^{-5} torr before deposition. Oxygen was used as the reactive gas. The selection of a partial oxygen pressure relative to Ar allowed us to fabricate tin films in oxidized states and regulate the film resistivity.

The first manufacturing operation of film deposition is sputtering of the target surface for 30 min. Then ion cleaning of the substrate was performed to improve the adhesion properties. A Zr-doped SnO₂ film was then deposited over several minutes until the necessary thickness was attained.

ST-50-0.6 glassceramic plates were used as substrates. The film composition was determined by electron-probe X-ray microanalysis by five measurements taken from various substrate segments with subsequent polynomial extrapolation of the composition over the substrate length. The samples formed by deposition were films with a thickness of 0.15–1.5 μm. The film thickness was measured using an MII-4

interferometer. To analyze the phase composition of the films, we performed X-ray structural studies using a Bruker D2 Phaser X-ray diffractometer. The results were processed using Bruker DIFFRAC EVA 3.0 software with the application of PDF2012 and TOPAS 4.2 databases. When measuring the temperature dependence of the resistivity, we used samples 9 mm in length sputtered onto a glassceramic substrate.

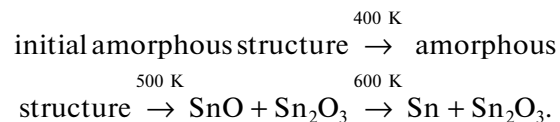
The resistivity measurements were performed using a two-probe potentiometric method. The absolute error of the temperature measurement was ± 1 K, while the relative error of the resistivity measurement was 0.5%.

3. EXPERIMENTAL RESULTS

3.1. Structure of Synthesized Films

The structure of Sn–Zr–O films was studied in [12]. It is shown that the film is amorphous in the initial state. The amorphous film crystallizes after heat treatment at 773 K for 17 h. The crystallite size depends on the zirconium concentration. The crystallite size decreases from 40 to 10 nm with an increase in the Zr content from 0.5 to 4.6 at %.

In contrast with [12], where heat treatment was performed in air, we performed thermal annealing of the films in a vacuum chamber under a residual pressure of no higher than 10^{-5} torr. This allowed us to compare structural transformations with the studied temperature dependences of the resistivity $\rho(T)$. The analysis of X-ray diffraction patterns of the synthesized films showed that the sample remains amorphous to a temperature of 673 K (curves 1, 2 in Fig. 1). The peaks observed in the dependences belong to the ST50-0.6 substrate material. The amorphous film crystallizes after heat treatment at 773 K for 30 min with the isolation of SnO crystallites of tetragonal structure of the P4/nmm symmetry space group (pdf 01-072-1012) and Sn₂O₃ of triclinic structure of the P-1 symmetry space group (pdf 00-025-1259) (curve 3 in Fig. 1). An increase in the treatment temperature (873 K for 30 min) leads to the isolation of metal tin of tetragonal structure of the I41/amd symmetry space group (pdf 01-089-4898) and disappearance of the SnO phase (curve 4 in Fig. 1). The chain of found transformations can be written as



3.2. Electrical Properties of the Synthesized Films

The above-described structural transformations of the Sn–Zr–O films should be reflected in the electro-transfer processes. In this context, we studied the temperature dependences of the resistivity of tin-oxide

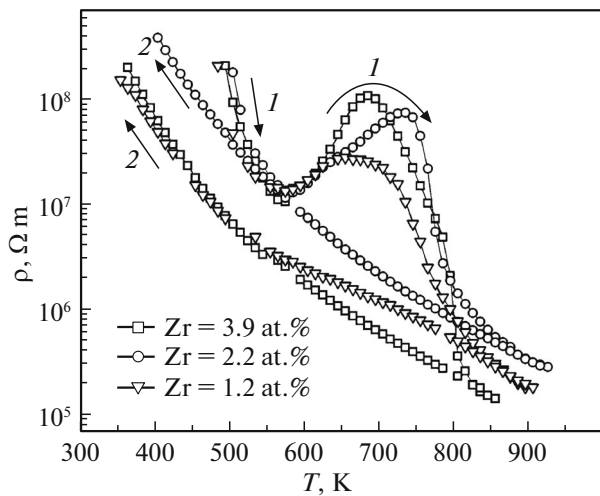


Fig. 2. Temperature dependences of the film resistivity upon heating (curve 1) and cooling (curve 2) in argon at $P = 380$ torr with various zirconium contents.

films with various contents of impurity atoms (Zr) (Fig. 2).

The analysis of our dependences showed that a peak is observed in the temperature range of 573–773 K ($\rho_{\max} \sim 673$ K). It should be noted that the degree of variation in the resistivity $\Delta\rho$ increases with an increase in the zirconium concentration in the film. After passing the maximal values of ρ , the resistivity rapidly decreases up to temperatures of the end of the thermal action (873 K). When cooling the sample, curves $\rho(T)$ are monotonic and approximated by the exponential dependence $\rho \sim \exp(1/T)$, which is characteristic of semiconductor materials.

The presence of a peak in the dependence $\rho(T)$ upon film heating can be explained when taking into account the experimental data of structural studies after heat treatment:

(i) the film structure remains amorphous in the temperature range from 573 to 673 K;

(ii) heat treatment at 773 K for 30 min leads to film crystallization with the isolation of Sn_2O_3 and SnO crystallites;

(iii) an increase in the annealing temperature (873 K for 30 min) transforms the SnO crystals into the oxide Sn_2O_3 and Sn;

(iv) no Zr-containing phase considerable for X-ray identification is revealed.

We can assume that the changes in short-range atomic order leading to an increase in the sample resistivity occur within the limits of an amorphous-film structure in the temperature range of 573 to 673 K. This process can be associated with structural relaxation of the amorphous structure in the films under study. A decrease in the resistivity as a factor of $\rho(T)$ above 673 K is associated with crystallization

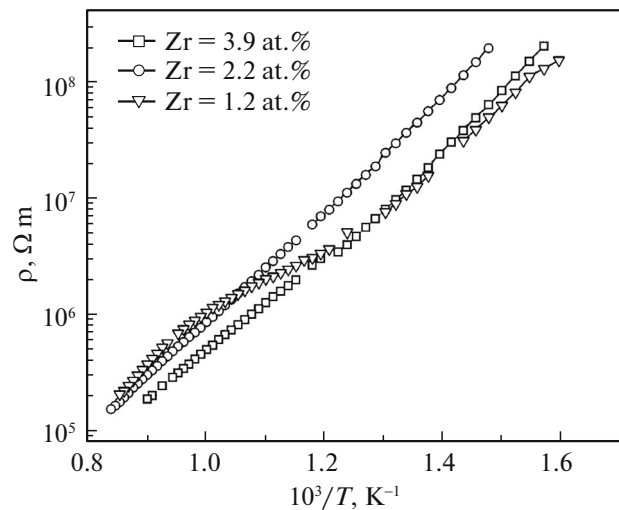


Fig. 3. Temperature dependences of the resistivity of films measured upon cooling in argon at $P = 380$ torr with various zirconium contents in the coordinates $\ln(\rho) = f(1/T)$.

processes. The lack of oxygen during film synthesis by the reaction method from a metallic target leads to the formation of phases of unsaturated tin oxide Sn_2O_3 and SnO. An increase in the degree of oxidation of metallic Sn atoms from SnO to Sn_2O_3 and the formation of metal phase crystals decreases the variation rate of $\rho(T)$.

When cooling the sample heated to 873 K, curves $\rho(1/T)$ are approximated by an exponential dependence. If the temperature dependence of the resistivity of the studied composites is described by the Arrhenius equation [14]:

$$\rho = \rho_0 \cdot \exp\left(-\frac{E_a^R}{2kT}\right), \quad (1)$$

where E_a^R is the activation energy of electrical conductivity, k is the Boltzmann constant, and T is the absolute temperature; then we can determine the activation energies of the conductivity E_a^R , which are presented in Table 1 for Sn–Zr–O films with various Zr contents, by experimental dependences (Fig. 3).

Analysis of the calculated activation energies showed that E_a^R is $\sim 0.78 \pm 0.05$ eV and is almost invariable with varying zirconium concentration. This

Table 1. Activation energy of the conductivity of Sn–Zr–O films depending on the Zr content after sample heating to 600 K

Zr concentration (at %)	Activation energy (eV)
3.9	0.78 ± 0.05
2.2	0.83 ± 0.05
1.2	0.73 ± 0.05

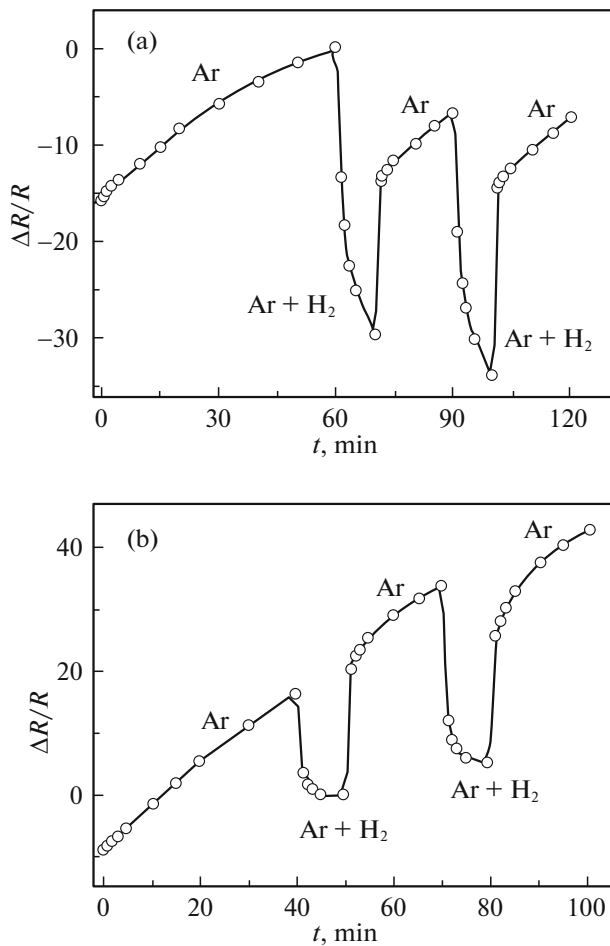


Fig. 4. Temporal dependences of the relative variation in the electrical resistance of the films of the Sn–Zr–O system with a Zr content of 2.2 at % at $T = 350$ K: (a) without coating and (b) with Pd deposited onto the surface.

value of the activation energy can be attributed to a donor level in the tin-oxide band gap formed by impurity zirconium atoms, which form substitutional defects in the crystal lattice.

3.3. Influence of Hydrogen on the Electrical Properties of Zr-Doped Sn–O Films

The above-considered structural and phase transformation during the heat treatment of thin-film Zr-doped tin oxide and related variations in the electrical properties should affect the formation of surface states in a wide-gap semiconductor upon the adsorption of atoms of various gases [12]. We measured the relative variation in the resistivity of the films under study in argon and with a hydrogen addition. The measurements were performed for samples preliminarily heat-treated at 873 K for 30 min.

We also studied the influence of the surface catalyst on the gas sensitivity of the films. The surface modification of Sn–Zr–O films was performed by catalyst

impurities under a microscope via the deposition of a microdroplet of an aqueous solution of palladium chloride (PdCl_2) with a known concentration onto the film surface. The aqueous solution contained 5% of palladium. After deposition, the droplet of the aqueous solution was dried at room temperature, and the samples were heated at 773 K for 30 min.

Figure 4 shows the results of studies of Sn–Zr–O films with a content of 2.2 at % Zr in Ar and with the addition of 7.6 torr of hydrogen into an inert medium. The temporal dependencies $\Delta R/R \cdot 100\%$ were calculated according to the equation

$$\frac{\Delta R}{R} = \frac{R - R_0}{R_0} \cdot 100\%, \quad (2)$$

where R_0 is the sample electrical resistance at the initial pressure or gas concentration and R is the sample electrical resistance during measurement at $T = 623$ K.

Curves in Fig. 4b correspond to the film with Pd preliminarily deposited onto the surface. It is seen that the presence of the catalyst does not affect the value of the gas sensitivity.

Palladium decreases the quantity $\Delta R/R \cdot 100\%$ with an increase in the Zr concentration. This is possible if we assume that Zr serves as the catalyst of adsorption processes in these films.

Zirconium most strongly affects the gas sensitivity of films at its concentration of ~ 1.2 at %. This is possibly associated with the formation of a solid solution of Zr in SnO_2 without the isolation of a separate phase.

The relative variation in the electrical resistance of the films of the Sn–O system increases with the addition of 0.6–3.9 at % Zr upon heating from 473 to 623 K.

It should be noted that the use of hydrogen as a probe gas for the Sn–Zr–O films arranged in air causes a more substantial variation than for the samples placed into an inert medium. The gas sensitivity of sensors based on tin oxide is determined by processes on the surface of grains constituting the film and affecting its conductivity. The most important are a variation in the oxygen vacancy concentration in the bulk due to exchange with the surface, the adsorption of particles from the gas phase inducing donor or acceptor levels, and the occurrence of chemical reactions on the grain surface leading to a variation in the population of adsorption centers [8].

To explain the variations in the electrical conductivity of a zirconium-containing tin oxide thin film upon contact with a gas medium of various compositions, the electron theory of chemisorption and catalysis based on surface electron states of semiconductors is applied [15]. Gas molecules adsorbed on an oxide surface can either give electrons (donors) or attach electrons from the oxide (acceptors). Zirconium-doped tin oxide is an n -type semiconductor, and the adsorption of acceptor molecules leads to the forma-

tion of near-surface regions depleted of electrons, which causes a decrease in the electrical conductivity. For example, this is the action of argon and air, which was observed during the exposure of a Sn–Zr–O film in argon (growth segments in Fig. 4). An electron-enriched surface layer is formed upon the adsorption of donor-type molecules on an *n*-type oxide, which increases the conductivity. This case is implemented upon hydrogen adsorption (decay segments in Fig. 4).

Thus, zirconium does not change the conductivity type of tin oxide in Zr–Sn–O systems and serves as a catalyst for the adsorption of molecular hydrogen, which can be associated with the presence of a zirconium solid solution in tin oxide.

4. CONCLUSIONS

Thin amorphous tin-oxide films doped with zirconium with a concentration from 0.6 to 3.9 at % were synthesized by ion-beam reactive sputtering. The onset of crystallization is observed upon heating thin-film Zr–Sn–O systems at 673 and 773 K, which is accompanied by the isolation of metastable phases SnO + amorphous phase and SnO + Sn₂O₃, which are subjected to substantial variations with further heating to 600 K converting into SnO + Sn₂O₃.

Such behavior can be associated with the fact that Zr forms solid solutions with tin oxide, which do not strongly affect the crystallization temperature but promote the formation of phases with unsaturated modifications of tin oxides.

It is established that after the crystallization of Zr-doped tin-oxide films at temperatures close to room temperature, electrotransfer is thermally activated with an activation energy of ~0.78 eV. The values of E_a^R for Zr–Sn–O films can be associated with donor levels formed by dissolved Zr atoms.

Tin oxide films with the addition of Zr from 0.6 to 3.9 at % manifest gas-sensor properties with respect to hydrogen after crystallization. Zirconium in Zr–Sn–O systems serves as the catalyst of the adsorption of molecular hydrogen, which can be associated with the presence of a zirconium solid solution in tin oxide.

ACKNOWLEDGMENTS

This study was supported by the Ministry of Education and Science of the Russian Federation within the scope of the project part of state order, project no. 3.1867.2017/4.6.

REFERENCES

1. A. Goetzberger and C. Hebling, *Sol. Energy Mater. Sol. Cells* **62**, 1 (2000).
2. P. Nelli, G. Faglia, G. Sverbeglieri, E. Cereda, G. Garbetta, A. Dieguez, A. R. Rodriguez, and J. R. Morante, *Thin Solid Films* **371**, 249 (2000).
3. L. S. Parshina, O. D. Khramova, O. A. Novodvorsky, A. A. Lotin, I. A. Petukhov, F. N. Putilin, and K. D. Shcherbachev, *Semiconductors* **51**, 407 (2017).
4. K. P. Bogdanov, D. Ts. Dimitrov, O. F. Lutskaia, and Yu. M. Tairov, *Semiconductors* **32**, 1033 (1998).
5. S. Monredon, A. Cellot, F. Ribot, C. Sanchez, L. Armelao, L. Gueneau, and L. Delattre, *J. Mater. Chem.* **12**, 2396 (2002).
6. N.-S. Baik, G. Sakai, N. Miura, and N. Yamazoe, *J. Am. Ceram.* **83**, 2983 (2000).
7. O. S. Makhdi, I. V. Malya, I. V. Sinev, S. B. Venig, and V. V. Kisin, in *Proceedings of the All-Russia, Saratov, Russia*, 2016, p. 34.
8. H.-W. Ha, K. Kim, M. de Borniol, and T. Toupance, *J. Solid State Chem.* **179**, 702 (2006).
9. E. S. Rembeza, O. Richard, and J. V. Landuyt, *Mater. Res. Bull.* **34**, 1527 (1999).
10. J. Rockenberger, U. zum Felde, M. Tischer, L. Troger, M. Haase, and H. Weller, *J. Chem. Phys.* **112**, 4296 (2000).
11. N. Sergent, P. Gelin, L. P. Camby, H. Praliaud, and G. Thomas, *Sens. Actuators*, **B 84**, 176 (2002).
12. S. I. Rembeza, E. S. Rembeza, T. V. Svistova, N. N. Kosheleva, and V. M. K. Al Tameemi, *Semiconductors* **49**, 1237 (2015).
13. S. A. Gridnev, Yu. E. Kalinin, A. V. Sitnikov, and O. V. Stognei, *Nonlinear Phenomena in Nano- and Microheterogeneous Systems* (BINOM, Labor. Znani, Moscow, 2012) [Moscow].
14. G. Bush, *Usp. Fiz. Nauk* **6**, 258 (1952).
15. A. M. Gas'kov and M. N. Rumyantseva, *Inorg. Mater.* **36**, 293 (2000).

Translated by N. Korovin